Fracture
A Topical Encyclopedia of Current Knowledge

Edited by Genady P. Cherepanov

CHAPTER 12

Failure of Pressurized Vessels

E. S. Folias

The chapter provides some basic results of the theoretical and experimental investigations of the failure criterion of a thin-walled vessel with a through crack taking into account effects of shell shape and curvature variations, and local yielding. The following plan is chosen to treat the subject.

Introduction
Section 1. General theory
Section 2. Formulation of the stress problem
Section 3. Stress distribution in the vicinity of a crack
Section 4. Effect of transverse vibrations
Section 5. Particular solutions
Section 6. General discussion
Section 7. Elastic brittle fracture criterion
Section 8. Plasticity correction
Section 9. Experimental verification
Conclusions
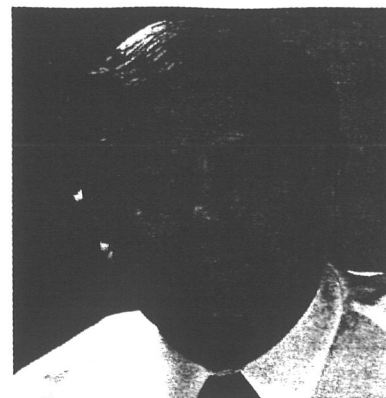
INTRODUCTION

In nature, shells are the rule rather than the exception. The list of natural shell-like structures is long, and the strength properties of some of them are remarkable. It is logical, therefore, for man to utilize them in his structures. However, to do this safely the designer must understand the fundamental laws that govern the strength and displacement characteristics of such structures, for they are not immune to failures, particularly in the fracture mode.

Moreover, we know from experience that thin-walled pressurized vessels do resemble balloons and like balloons are subject to puncture and explosive loss. For a given material, under a specified stress field, e.g. due to an internal pressure, there exists a minimum crack length in the material which will become self-propagating. Crack lengths less than the critical value will cause leakage, but not destruction. However, if the critical crack length is ever reached, either by penetration or by the growth of a small fatigue crack, an explosion and complete loss of the structure may occur. Similarly, for a given crack length, there will be a critical internal pressure beyond which the pressure vessel will fail catastrophically. One conjectures, therefore, that there exists a certain relationship between internal pressure and crack size. More specifically, one may expect that the following will be true:

$$q_{\text{critical}} = F \{\text{shell geometry, flaw shape, flaw size, loading, material properties, other}\}. \quad (1)$$

The subject of our concern, therefore, is the derivation of an equation that relates the critical pressure to the critical crack length in a pressurized vessel, based upon analytical considerations. A relation of this type is called fracture criterion.

For the derivation of a fracture criterion, two ingredients are necessary: the knowledge of the stress distribution due to the presence of a crack, and an energy balance for crack initiation. Accordingly, in

E. S. FOLIAS

the first part of this chapter, a review of past work on initially curved sheets dealing with the stress distribution in the vicinity of a crack is given, and in the second part a fracture criterion which may be used to predict fracture in pressurized vessels is presented. Finally, comparison of the theoretically predicted values with some of the existing experimental data substantiates the validity of this derivation and its potential use.

1. GENERAL THEORY

In the following, we shall consider bending and stretching of thin shallow shells, as illustrated in Fig. 1 and described by the traditional two-dimensional linear theory. Such a theory is appropriate in view of the "thinness" of the shell. We shall limit our considerations to linearly elastic, isotropic, homogeneous, constant thickness, shallow segments of shells, that are subjected to small deformations.

The basic variables in the theory of shallow shells are the displacement function $w(x,y)$, in the direction of the z axis (see Fig. 1), and the stress function $F(x,y)$ that represents the stress resultants tangent to the middle surface of the shell. Following Marguerre (1938), the coupled differential equations governing w and F, with x and y as the rectangular Cartesian coordinates of the base plane, are given by:

$$\nabla^4 F = Eh\left[2\frac{\partial^2 w_0}{\partial x \partial y}\frac{\partial^2 w}{\partial x \partial y} - \frac{\partial^2 w_0}{\partial x^2}\frac{\partial^2 w}{\partial y^2} - \frac{\partial^2 w_0}{\partial y^2}\frac{\partial^2 w}{\partial x^2}\right] \tag{2}$$

$$D\nabla^4 w = -q - 2\frac{\partial^2 F}{\partial x \partial y}\frac{\partial^2 w_0}{\partial x \partial y} + \frac{\partial^2 F}{\partial x^2}\frac{\partial^2 w_0}{\partial y^2} + \frac{\partial^2 F}{\partial y^2}\frac{\partial^2 w_0}{\partial x^2}, \tag{3}$$

where $w_0(x,y)$ describes the initial shape of the shell in reference to that of a flat plate, E is Young's modulus, D is the flexural rigidity, h is the shell thickness, and q is the internal pressure.

2. FORMULATION OF THE STRESS PROBLEM

Let us consider a portion of a thin, shallow shell, of constant thickness h, subjected to an internal pressure $q(x,y)$ and containing a crack of length $2c$ (see Fig. 1). Our problem is to find two functions $F(x,y)$ and $w(x,y)$ which satisfy the differential equations 2 and 3, together with the appropriate boundary conditions. More specifically, along the faces of the crack, we require the normal moment,
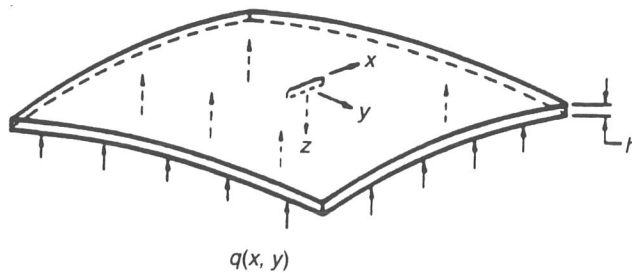
equivalent shea
crack, we requi

It is evide
initial curvature
a spherical and
Alternatively, f
proper superpo

3. STRESS D

Two simp
cylindrical, wh

(i) Spherical

For a shal

Substituting E

It is wortl
shell tends to i
cover precisely
shell radius, th
stretching load
natively, a ben

For a sphe
Folias, 1965a)
Their solution

with ν being P
series solution

It is clear
matter, if one
$(R/h) < 10^3$,
cases, howeve
indeed justifia

Without
symmetrical l

$q(x, y)$

FIGURE 1. Initially curved sheet containing a finite line crack.

equivalent shear and normal and tangential membrane forces to vanish. Similarly, far away from the crack, we require that the appropriate loading and support conditions be satisfied.

It is evident from Eqs. 2 and 3 that a theoretical attack of the general problem with an arbitrary initial curvature presents formidable mathematical complexities. However, for the simple geometries of a spherical and a cylindrical shell, exact analytical solutions have been obtained in an asymptotic form. Alternatively, for other more complicated shell geometries, good approximations can be obtained by a proper superposition of the above two solutions.

3. STRESS DISTRIBUTION IN THE VICINITY OF A CRACK

Two simple geometries of pressurized vessels immediately come to mind: a spherical and a cylindrical, which are considered below.

(i) Spherical Shell

For a shallow spherical shell the radius of curvature remains constant in all directions; therefore,

$$\frac{\partial^2 w_0}{\partial x \partial y} = 0; \qquad \frac{\partial^2 w_0}{\partial x^2} = \frac{\partial^2 w_0}{\partial y^2} = \frac{1}{R}. \tag{4}$$

Substituting Eq. 4 into Eqs. 2 and 3 one obtains the well known Reissner's equations:

$$\frac{Eh}{R} \nabla^2 w + \nabla^4 F = 0, \tag{5}$$

$$\nabla^4 w - \frac{1}{RD} \nabla^2 F = -\frac{q}{D}. \tag{6}$$

It is worthy to note that the above governing equations are coupled and that, as the radius of the shell tends to infinity, they become uncoupled. This suggests, therefore, that, in the limit, one must recover precisely the corresponding solution to the case of a flat plate. On the other hand, for an arbitrary shell radius, the coupling of the equations suggests that there exists an interaction between bending and stretching loads. That is, a stretching load will induce both stretching and bending stresses. Alternatively, a bending load will also induce both stretching and bending stresses.

For a spherical cap which contains at the apex a crack of finite length $2c$ (see Fig. 2), the author (see Folias, 1965a) has reduced the problem to that of the solution of two coupled singular integral equations. Their solution was then sought in the form of a power series in λ^2, where λ^2 is defined by:

$$\lambda^2 = \{12(1 - \nu^2)\}^{1/2} \frac{c^2}{Rh}, \tag{7}$$

with ν being Poisson's ratio. It may also be noted that, for λ less than a certain calculated bound, this series solution has been shown to converge to the exact solution (see Folias, 1964a).

It is clear from Eq. 7 that λ is small for large ratios of R/h and small crack lengths. As a practical matter, if one considers crack lengths less than one-tenth of the periphery, i.e. $2c < (2pR/10)$, and for $(R/h) < 10^3$, a corresponding upper bound for λ can be obtained, i.e. $\lambda < 20$. For most practical cases, however, the range is $0 < \lambda < 3$. Consequently, an asymptotic expansion for small values of λ is indeed justifiable.

Without getting into the mathematical details, the stress distribution around the crack tip for symmetrical loadings is given by:
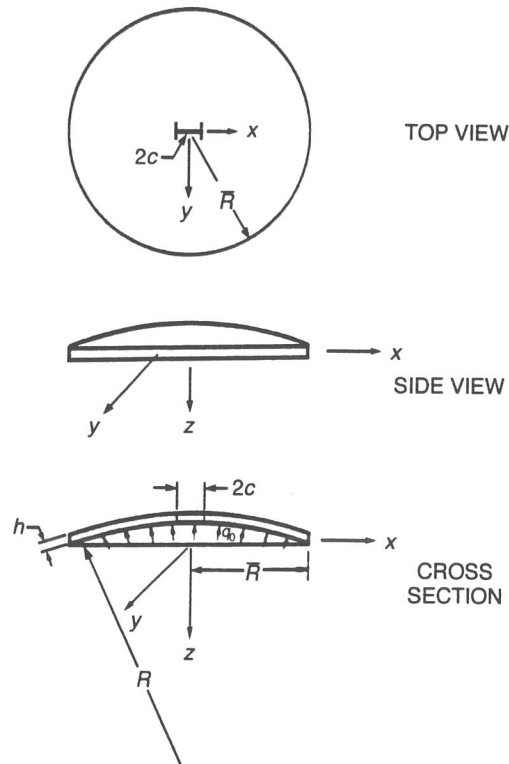
FIGURE 2. Geometrical configuration of a pressurized spherical cap.

Extentional Stresses (valid through the thickness):

$$\sigma_{xx}^{(e)} = P_s^{(e)} \left(\frac{c}{2r}\right)^{1/2} \left(\frac{3}{4}\cos\frac{\theta}{2} + \frac{1}{4}\cos\frac{5\theta}{2}\right) + O(r^o) \tag{8}$$

$$\sigma_{yy}^{(e)} = P_s^{(e)} \left(\frac{c}{2r}\right)^{1/2} \left(\frac{5}{4}\cos\frac{\theta}{2} - \frac{1}{4}\cos\frac{5\theta}{2}\right) + O(r^o) \tag{9}$$

$$\tau_{xy}^{(e)} = P_s^{(e)} \left(\frac{c}{2r}\right)^{1/2} \left(-\frac{1}{4}\sin\frac{\theta}{2} + \frac{1}{4}\sin\frac{5\theta}{2}\right) + O(r^o), \tag{10}$$

Bending Stresses (valid on the "tension side" of the shell):

$$\sigma_{xx}^{(b)} = P_s^{(b)} \left(\frac{c}{2r}\right)^{1/2} \left(-\frac{3 - 3\nu}{4}\cos\frac{\theta}{2} - \frac{1 - \nu}{4}\cos\frac{5\theta}{2}\right) + O(r^o) \tag{11}$$

$$\sigma_{yy}^{(b)} = P_s^{(b)} \left(\frac{c}{2r}\right)^{1/2} \left(\frac{11 + 5\nu}{4}\cos\frac{\theta}{2} + \frac{1 - \nu}{4}\cos\frac{5\theta}{2}\right) + O(r^o) \tag{12}$$

$$\tau_{xy}^{(b)} = P_s^{(b)} \left(\frac{c}{2r}\right)^{1/2} \left(-\frac{7 + \nu}{4}\sin\frac{\theta}{2} - \frac{1 - \nu}{4}\sin\frac{5\theta}{2}\right) + O(r^o) \tag{13}$$

where:

$$P_s^{(e)} = \sigma^{(e)} \left(1 + \frac{3\pi}{32}\lambda^2\right) + \sigma^{(b)} \frac{\lambda^2}{\sqrt{3}} \frac{(1 - \nu^2)^{1/2}}{3 + \nu} \left\{\frac{7}{32} + \frac{3}{8}\left[\gamma + \ln\frac{\lambda}{4}\left(\gamma + \ln\frac{\lambda}{4}\right)\right]\right\} + O(\lambda^4 \ln\lambda), \tag{14}$$

and

$$P_s^{(b)} = -\sigma^{(e)}\frac{\lambda^2\sqrt{3}}{(3+\nu)(1-\nu^2)^{1/2}}\left\{\frac{1+7\nu}{32} + \frac{1+3\nu}{8}\left(\gamma + \ln\frac{\lambda}{4}\right)\right\} - $$
$$- \sigma^{(b)}\frac{1}{3+\nu}\left(1 + \frac{1+3\nu}{3+\nu}\frac{\pi\lambda^2}{32}\right) + O\left(\lambda^4\ln\frac{\lambda}{4}\right),$$

(15)

where $\lambda = 0.577$ is Euler's constant.

Finally, it should be emphasized that the stress coefficients in Eqs. 14 and 15 contain only up to $O(\lambda^2)$ terms. Their use, therefore, is limited to only small values of the parameter λ, i.e. for $\lambda < 1$. For larger values of λ, it is necessary to consider higher-order terms in order to guarantee the convergence of the solution. Thus, for a Poisson's ratio of $\frac{1}{3}$, an alternative form of the stress coefficients good up to $\lambda < 6$ is given by:

$$P_s^{(e)} = \sigma^{(e)}A_s^{(e)} - 0.54\sigma^{(b)}a_s^{(e)}$$

(16)

$$P_s^{(b)} = 1.81\sigma^{(e)}a_s^{(b)} - 0.30\sigma^{(b)}A_s^{(b)},$$

(17)

where the coefficients may now be approximated by:

$$A_s^{(e)} = \sqrt{1 + 0.3295\lambda^2}, \qquad a_s^{(e)} = 0.0002 + 0.0580\lambda - 0.0042\lambda^2$$

(18)

$$A_s^{(b)} = 0.993 + 0.032\lambda, \qquad a_s^{(b)} = -0.0080 + 0.0550\lambda - 0.0010\lambda^2 - 0.0005\lambda^3.$$

(19)

(ii) Flat Plate

A flat plate represents the degenerate case of a spherical cap whereby the radius becomes infinite, thus:

$$\frac{\partial^2 w_0}{\partial x\partial y} = \frac{\partial^2 w_0}{\partial x^2} = \frac{\partial^2 w_0}{\partial y^2} = 0.$$

(20)

Substituting Eq. 20 into Eqs. 2 and 3, one recovers the classical flat plate equations:

$$\nabla^4 F = 0$$

(21)

$$\nabla^4 w = -\frac{q}{D}.$$

(22)

The problem of a flat plate containing a finite line crack and subjected to a lateral load has been investigated by many authors for various types of loadings. The solution, however, may also be obtained from the "spherical cap" solution by simply letting $R \to \infty$, or $\lambda \to \infty$. Thus the stresses around the crack tip are given precisely by Eqs. 8–13, where the stress coefficients now become:

$$P_p^{(e)} = \sigma^{(e)} \qquad \text{and} \qquad P_p^{(b)} = -\frac{1}{3+\nu}\sigma^{(b)}.$$

(23)

(iii) Cylindrical Shell

For a shallow cylindrical shell, one of the principal radii of curvatures is infinite, while the other is constant; therefore:

$$\frac{\partial^2 w_0}{\partial x\partial y} = \frac{\partial^2 w_0}{\partial x^2} = 0, \qquad \frac{\partial^2 w_0}{\partial y^2} = \frac{1}{R}.$$

(24)

(8)

(9)

(10)

(11)

(12)

(13)

$\ln\lambda),$ (14)

Substituting Eq. 24 into Eqs. 2 and 3, one recovers the governing equations for a shallow cylindrical shell, i.e.:

$$\frac{Eh}{R}\frac{\partial^2 w}{\partial x^2} + \nabla^4 F = 0, \tag{25}$$

$$\nabla^4 w - \frac{1}{RD}\frac{\partial^2 F}{\partial x^2} = -\frac{q}{D}. \tag{26}$$

There are two cases of special interest that immediately come to mind: an axial crack and a peripheral crack. Due to the mathematical complexities of this problem, Sechler and Williams (1959) suggested an approximate yet very clever method of solution based upon the behavior of a beam on an elastic foundation, and thus they were able to obtain reasonable agreement with some of the experimental results. In their simplified model, they theorized that curvature plays the same role as an elastic foundation. Subsequently, using the same method of solution as in Folias (1965a), the author was able to study this problem from a slightly more sophisticated point of view, and the mathematical details for an axial, as well as a peripheral line crack (see Fig. 3), can be found in the literature (Folias, 1965b and 1967).

A few years later, two more theoretical analyses of the same problem appeared in literature, the axial crack was investigated by Copley and Sanders (1969) and the peripheral crack was investigated by Duncan and Sanders (1969). Their method of solution consisted of the application of the Fourier Integral Transforms leading to the derivation of two coupled singular integral equations (different in form from the author's), which in turn were approximated to high accuracy via matrix equations and were subsequently solved with the aid of a computer. Their results were based on a zero "applied
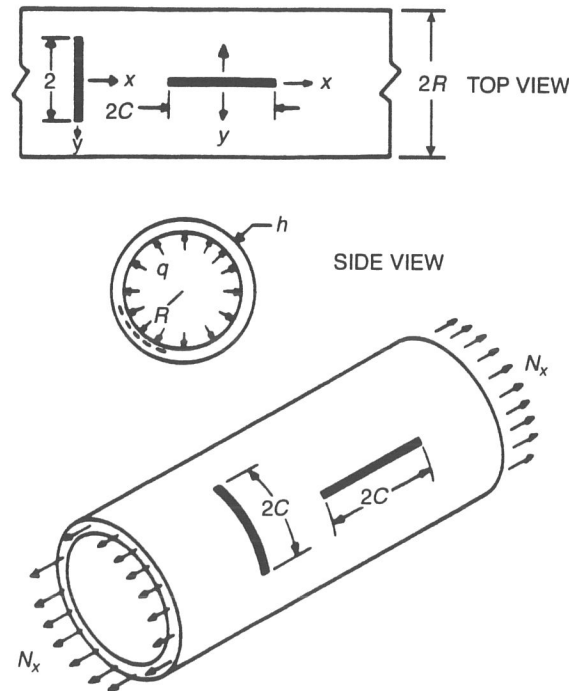
bending" load, i
author's findings
Again omitt
around the crack
For an axia

$$P_{c,a}^{(e)} = \sigma^{(e)}($$

$$+ ($$

$$P_{c,a}^{(b)} =$$

or the alternativ

where:

$$A_{c,a}^{(e}$$
$$A_{c,a}^{(b}$$
$$a_{c,a}^{(e)}$$
$$a_{c,a}^{(b)}$$

Here again, the
by Erdogan and
For a peri

$$P_{c,p}^{(e)} = \sigma^($$

$$+$$

$$P$$

*Erdogan and K
larger range of

FIGURE 3. Geometrical configuration of an axially and peripherally cracked cylindrical shell subject to an axial extension N_X, and an internal pressure q_0.

bending" load, i.e. $\sigma^{(b)} = 0$, and for a Poisson's ratio of $\nu = 0.32$. Their results are consistent with the author's findings.

Again omitting the long and tedious mathematical details (see Folias, 1965b and 1967), the stresses around the crack tip are given by Eqs. 8–13, where the stress coefficients become:

For an axial crack:

$$P_{c,a}^{(e)} = \sigma^{(e)}\left(1 + \frac{5\pi\lambda^2}{64}\right) - \sigma^{(b)}\frac{\lambda^2}{\sqrt{3}}\frac{(1-\nu^2)^{1/2}}{3+\nu}\left\{\frac{5+37\nu}{96(1-\nu)} + \frac{1+5\nu}{16(1-\nu)}\left(\gamma + \ln\frac{\lambda}{8}\right)\right\} + $$
$$+ O(\lambda^4\ln\lambda) \tag{27}$$

$$P_{c,a}^{(b)} = -\sigma^{(e)}\frac{\sqrt{3}\lambda^2}{(1+\nu^2)^{1/2}}\frac{1}{(3+\nu)}\left\{\frac{5+37\nu}{96} + \frac{1+5\nu}{16}\left(\gamma + \ln\frac{\lambda}{8}\right)\right\} - $$
$$-\sigma^{(b)}\frac{1}{3-\nu}\left\{1 - \frac{1+2\nu+5\nu^2}{(3+\nu)(1-\nu)}\frac{\pi\lambda^2}{64}\right\} + O(\lambda^4\ln\lambda); \quad \text{for } \lambda < 1, \tag{28}$$

or the alternative approximate expressions valid for $\nu = \frac{1}{3}$:

$$P_{c,a}^{(e)} = \sigma^{(e)}A_{c,a}^{(e)} - 0.54\sigma^{(b)}a_{c,a}^{(e)}, \tag{29}$$

$$P_{c,a}^{(b)} = 1.81\sigma^{(e)}a_{c,a}^{(b)} - 0.30\sigma^{(b)}A_{c,a}^{(b)}, \tag{30}$$

where:

$$A_{c,a}^{(e)} = 0.8097 + 0.4110\lambda + 0.0071\lambda^2, \tag{31}$$

$$A_{c,a}^{(b)} = 1.0188 - 0.0541\lambda + 0.0016\lambda^2, \tag{32}$$

$$a_{c,a}^{(e)} = -0.0093 + 0.0701\lambda - 0.0077\lambda^2 + 0.0003\lambda^3, \tag{33}$$

$$a_{c,a}^{(b)} = 0.0073 - 0.0029\lambda + 0.0422\lambda^2 - 0.0190\lambda^3 + 0.0028\lambda^4 - 0.0001\lambda^5. \tag{34}$$

Here again, the stress coefficients are approximate functions of λ and are similar to the results obtained by Erdogan and Kibler* (1969) as well as by Copley and Sanders (1969).

For a peripheral crack:

$$P_{c,p}^{(e)} = \sigma^{(e)}\left(1 + \frac{\pi\lambda^2}{64}\right) + \sigma^{(b)}\frac{\lambda^2}{\sqrt{3}}\frac{(1-\nu^2)^{1/2}}{(3+\nu)}\left\{\frac{(1+\nu)}{32(1-\nu)} + \frac{(1+\nu)}{16(1-\nu)}\left(\gamma + \ln\frac{\lambda}{8}\right)\right\} + $$
$$+ O(\lambda^4\ln\lambda) \tag{35}$$

$$P_{c,p}^{(b)} = -\sigma^{(e)}\frac{\sqrt{3}\lambda^2}{(1-\nu^2)^{1/2}}\frac{1}{(3+\nu)}\left\{\frac{1+\nu}{32} + \frac{1+\nu}{16}\left(\gamma + \ln\frac{\lambda}{8}\right)\right\} - $$
$$- \sigma^{(b)}\frac{1}{3+\nu}\left\{1 - \frac{5+2\nu+\nu^2}{(3+\nu)(1-\nu)}\frac{\pi\lambda^2}{64}\right\} + O(\lambda^4\ln\lambda) \tag{36}$$

$$P_{c,p}^{(e)} = \sigma^{(e)}\frac{1}{\Delta}\left\{1 + \frac{5+2\nu+\nu^2}{(1-\nu)(3+\nu)}\frac{\pi\lambda^2}{64} - \frac{19-2\nu-\nu^2}{32(1-\nu)(3+\nu)}\left(\frac{\lambda}{4}\right)^4 + \right.$$
$$\left. + \frac{23+22\nu+11\nu^2}{8(1-\nu)(3+\nu)}\left(\gamma + \ln\frac{\lambda}{8}\right)\left(\frac{\lambda}{4}\right)^4\right\} + $$
$$+ \frac{\sqrt{12(1-\nu)^2}}{32(3+\nu)}\frac{(1+\nu)}{(1-\nu)}\frac{1}{\Delta}\sigma^{(b)}\lambda^2\left\{1 + 2\left(\gamma + \ln\frac{\lambda}{8}\right) - \frac{11\pi}{16}\left(\frac{\lambda}{4}\right)^2\right\} \tag{37}$$

---

*Erdogan and Kibler used the Folias formulation and method of solution, but extended the numerical results to a larger range of values for the parameter λ.

$$P_{c,p}^{(b)} = \sigma^{(e)}\frac{3(1+\nu)}{16(3+\nu)\sqrt{12(1-\nu)^2}}\frac{\lambda^2}{\Delta}\left\{1 + 2\left(\gamma + \ln\frac{\lambda}{8}\right) - \left(\frac{17-22\nu-11\nu^2}{16(1-\nu)}\right)\pi\left(\frac{\lambda}{4}\right)^2\right\} +$$

$$+ \sigma^{(b)}\frac{1}{(3+\nu)\Delta}\left\{1 - \frac{\pi\lambda^2}{64} + \frac{13+2\nu+\nu^2}{32(3+\nu)(1-\nu)}\left(\frac{\lambda}{4}\right)^4 + \right. \tag{38}$$

$$\left. + \frac{-25+22\nu+11\nu^2}{8(3+\nu)(1-\nu)}\left(\gamma + \ln\frac{\lambda}{8}\right)\left(\frac{\lambda}{4}\right)^4\right\}$$

where

$$\Delta = 1 + \frac{(1+\nu)^2}{(1-\nu)(3+\nu)}\frac{\pi\lambda^2}{32} - \left[\frac{14+12\nu+6\nu^2}{32(1-\nu)(3+\nu)} + \frac{5+2\nu+\nu^2}{16(1-\nu)(3+\nu)}\pi^2\right]\left(\frac{\lambda}{4}\right)^4 +$$

$$+ \frac{-35+50\nu+25\nu^2}{4(1-\nu)(3+\nu)}\left(\gamma + \ln\frac{\lambda}{8}\right)\left(\frac{\lambda}{4}\right)^4 - \frac{(1+\nu)^2}{(1-\nu)(3+\nu)}\left(\gamma + \ln\frac{\lambda}{8}\right)^2\left(\frac{\lambda}{4}\right)^4. \tag{39}$$

4. EFFECT OF TRANSVERSE VIBRATIONS

In addition to the usual external applied loads, pressure vessels are frequently subjected to lateral vibrations. In order to establish what effect if any such vibrations have on the mechanism of fracture, an investigation was undertaken (see Do and Folias, 1971). The analysis revealed that, in general, transverse vibrations reduce the amplitude of the stress intensity factor. However, when the forcing frequency approaches the local natural frequency of the uncracked shell, the stress intensity factor increases without bound. This phenomenon, coupled with the usual $l/\sqrt{r}$ singular behavior, causes the pressure vessel to fail at even lower nominal values of the internal pressure. Consequently, a designer must take into account the presence of transverse vibrations in structures, for they may have severe implications on the mechanisms of failure common in such applications as aging aircraft, turbines, etc.

5. PARTICULAR SOLUTIONS

In general, the actual stress fields are dependent upon the contributions of the particular solutions reflecting the magnitude and distribution of the applied loads. On the other hand, the singular part of the solution, that is the terms producing infinite elastic stresses at the crack tip, will depend upon the local stresses existing along the vicinity of the crack before it is cut, which of course are precisely the stresses that must be removed by the particular solutions described above in order to obtain the stress-free edges as required physically.

(i) Clamped Spherical Shell

Consider a clamped segment of a shallow spherical shell of a base radius R_O and containing at its apex a radial crack of finite length $2c$ (see Fig. 4). The shell is subjected to a uniform internal pressure q_0, with a radial tension of $N_r = (q_0/2)R$ and, because it is clamped, we require that the displacement and slope vanish at $R = R_O$. For this problem, the residual *applied bending* and *applied stretching* loads at the crack faces become: $\sigma^{(b)} = 0$ and $\sigma^{(e)} = q_0R/(2h)$.

(ii) Closed Cylindrical Tank

Consider a shallow cylindrical shell containing a crack of length $2c$. The shell is subjected to a uniform internal pressure q_0, with an axial tension of $N_x = (q_0R/2)$, $M_y = 0$, far away from the crack. For this problem, if the crack is parallel to the cylinder axis, then $\sigma^{(b)} = 0$ and $\sigma^{(e)} = q_0R/h$.
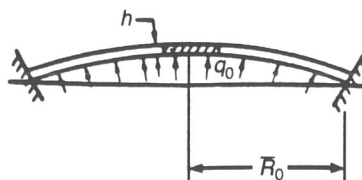
$\biggl)^2\biggr\} +$

(38)

$+$

(39)

FIGURE 4. Pressurized spherical cap with fixed ends.

On the other hand, if the crack is perpendicular to the cylinder axis, then $\sigma^{(b)} = 0$ and $\sigma^{(e)} = q_0 R/(2h)$.

6. GENERAL DISCUSSION

It becomes evident from the above analysis that in an initially curved sheet the stresses near the crack tip possess the usual $1/\sqrt{r}$ singular behavior which is characteristic of two dimensional linear elastic problems. Moreover, the angular distribution around the crack tip is precisely the same as that of a flat plate and that the initial curvature appears only when stress intensity factors are considered. They appear in such a way that, within limits, one can recover precisely the flat plate behavior.

Thus, the general effect of a positive (negative) initial curvature, in reference to that of a flat plate, is to increase (decrease) the stresses in the neighborhood of the crack tip and to reduce (increase) its resistance to fracture initiation. For a cylindrical shell with an axial crack, for example, one has:

$$\frac{\sigma_{\text{hoop}}}{\sigma_{\text{plate}}} = \frac{1}{\sqrt{1 + 0.317\lambda^2}},$$

(40)

which correlates flat plate behavior with that of initially curved specimens. In experimental work, for example, considerable savings can be realized, for one would be able to design pressure vessels based on experiments carried out on flat plates.

7. ELASTIC BRITTLE FRACTURE CRITERION

From the foregoing discussion, it becomes apparent that initially curved sheets which contain through flaws or cracks present a reduced resistance to fracture initiation. Consequently, the presence of a flaw or a crack in the walls of a pressure vessel can severely reduce the strength of the structure and can cause sudden failure at nominal tensile stresses less than the material yield strength. To ensure, therefore, the integrity of a structure, the designer must be cognizant of the relation that exists between fracture load, materials properties, flaw shape and size and structural geometry.

The principal task, however, of fracture mechanics is precisely the prediction of failure due to the presence of sharp discontinuities. Specifically, the approach is based on a corollary of the first law of thermodynamics which was first applied to the phenomenon of fracture by Griffith (1924). His hypothesis was that the total energy of a cracked system subjected to external loading remains constant as the crack extends an infinitesimal distance. That is:

$$\frac{\partial U_{\text{system}}}{\partial c} = 0.$$

(41)

E. S. FOLIAS

Following the work of Griffith, the total energy of the system is given by:

$$U_{system} = U_{loading} + U_{surface} + U_{strain},$$ (42)

where the increase in strain energy due to the presence of a line crack may be calculated by considering the discontinuity in the v-displacement across the crack. For example, in the case of a crack that is subjected to a Mode I loading this becomes:

$$U_{strain} = -\tfrac{1}{2} \int_{-c}^{c} \sigma_y(x, 0)(v^+ - v^-)\, dx,$$ (43)

which, in view of the previous results, now becomes:

$$U_{strain} = -\frac{\pi}{E} c\{[P^{(e)}]^2 + \tfrac{2}{3}(1 + \nu)^2[P^{(b)}]^2\}.$$ (44)

Thus, for crack instability, we have:

$$4\gamma = -\frac{\partial U_{strain}}{\partial c},$$ (45)

where γ is the surface energy per unit area. Substituting Eq. 44 into Eq. 45 one finds:

$$4\gamma = \frac{2\pi c}{E}\{[P^{(e)}]^2 + \tfrac{2}{3}(1 + \nu)^2[P^{(b)}]^2\} + 2\frac{\pi}{E}c^2\left\{P^{(e)}\frac{dP^{(e)}}{dc} + \tfrac{2}{3}(1 + \nu)^2 P^{(b)}\frac{dP^{(b)}}{dc}\right\} = \frac{2K_{Ic}^2}{E},$$ (46)

where K_{Ic} is the plane stress fracture toughness in mode I. The reader may notice that, in the limit, as $R \to \infty$ the elastic fracture criterion for flat plates is recovered.
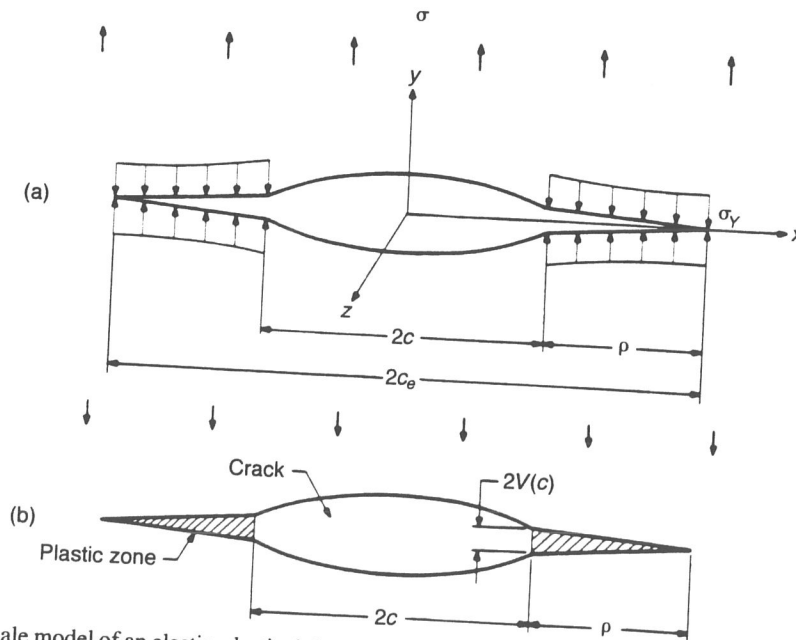

FIGURE 5. Dugdale model of an elastic-plastic deformation near a crack of length $2c$ and subject to a tensile loading.

8. PLASTICITY CORRECTION

Due to the presence of high stresses in the vicinity of the tip of a crack, when the appropriate yield criterion is satisfied, localized plastic deformation occurs and a plastic zone is created. This phenomenon effectively increases the crack length and therefore must be accounted for. Following Dugdale (1960), the size of the plastic zone (see Fig. 5) may be approximated by:

$$\frac{c}{c_e} = \cos\frac{\pi\sigma}{2\sigma_\gamma}, \tag{47}$$

where c_e now represents the effective crack length and σ_y the uniaxial tension yield stress. Thus, introducing a correction factor that accounts for plasticity effects, one finds the following approximate fracture criterion:

$$\cos\left[\sigma^{(e)}([P^{(e)}]^2 + \frac{33 + 6\nu - 7\nu^2}{3(9 - 7\nu)}(1 + \nu)[P^{(b)}]^2)\frac{\pi}{2\sigma_\gamma}\right] = \exp\left(-\frac{\pi K^2}{8\sigma_\gamma^2}\frac{1}{c}\right). \tag{48}$$

In general, the stress coefficients $P^{(e)}$ and $P^{(b)}$ are functions of the crack size, shell geometry, material properties and loading characteristics. For certain simple loadings, however, the table below gives a fairly good approximation of the stress coefficients:

Long cylinder axial crack

$$P^{(e)} = \sqrt{1 + 0.317\lambda^2}\left(\frac{q_0 R}{h}\right)$$

$$P^{(b)} = 0$$

Long cylinder peripheral crack

$$P^{(e)} = \sqrt{1 + 0.05\lambda^2}\left(\frac{q_0 R}{2h}\right)$$

$$P^{(b)} = 0$$

Spherical cap

$$P^{(e)} = \sqrt{1 + 0.466\lambda^2}\left(\frac{q_0 R}{2h}\right)$$

$$P^{(b)} = 0$$

9. EXPERIMENTAL VERIFICATION

In judging the adequacy of a theory, one often compares theoretical and experimental results. For this reason, in Fig. 6 we compare the theoretically predicted values (Eq. 40) with the experimental data obtained by Kihara, Ikeda and Iwanaga (1966) on cylindrical pipes containing axial notches. The reader may note that the theoretically predicted values are somewhat conservative (as they should be) and are fairly well vindicated by the experimental data. Thus, one may conclude that Eq. 40 may be used to predict the response behavior of curved sheets from corresponding flat sheet test data. As a practical matter, the use of such a property offers to designers and to manufacturers potentially substantial economic savings.

Next, we compare our results with a set of data obtained by Anderson and Sullivan for a 6 in. diameter, 0.060 in. thick, cylinders of 2014-T6 aluminum tested at $-320°F$. However, in order to utilize Eq. 48, one must know a priori the material fracture toughness K_c. For this reason, we use one of the
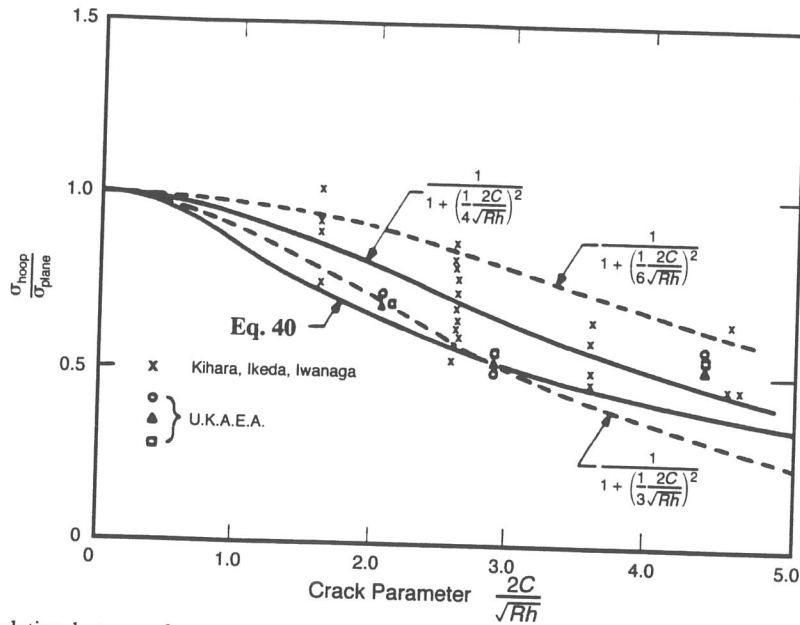
E. S. FOLIAS

FIGURE 6. Correlation between fracture stress ratio of a cylindrical shell and that of a flat plate versus the ratio $(2cl/\sqrt{Rh})$.

data points, e.g. the first one, to compute K_c. This value is then used in conjunction with Eq. 48 to predict the remaining failing hoop stresses. The results are shown in Fig. 7. The agreement is very good. Moreover, results of tests on 6 in. diameter, 0.020 in. thick cylinders made out of 5Al-2.5Sn-Ti, with full thickness cracks, also show a very good agreement (see Fig. 8).

Similarly, comparison between the theoretical and experimental data obtained by Sopher et al. (1959) for 9 in. diameter, $\frac{3}{4}$ in. thickness spheres with through-cracks is given in Fig. 9. Here too, the comparison is very good.
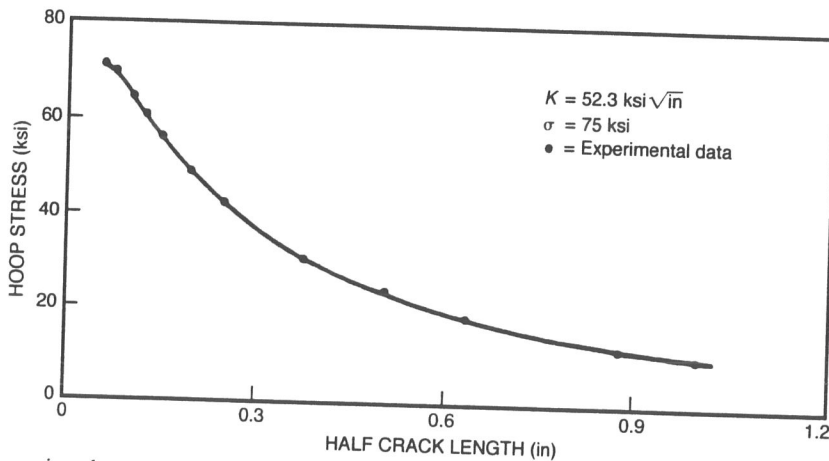

FIGURE 7. Comparison between theory and experiment for 2014-T6 aluminum cylindrical pressure vessels at room temperature.
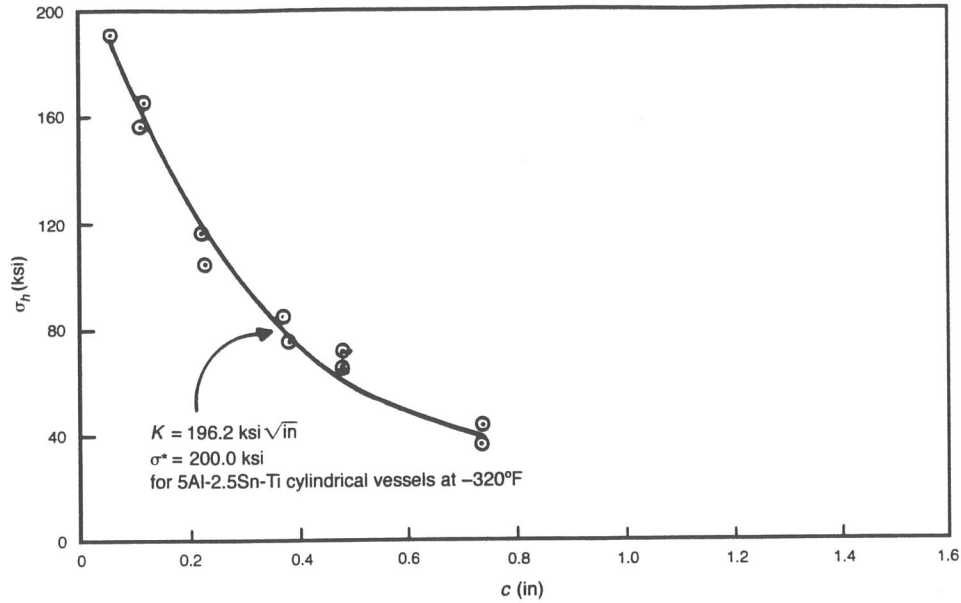
FIGURE 8. Comparison between theory and experiment for 5Al-2.5Sn-Ti cylindrical pressure vessels at −320°F.

CONCLUSIONS

In view of the above, one concludes that the general effect of an initial curvature, in reference to that of a flat plate, is to increase the stresses in the neighborhood of the crack point and thus reduce its resistance to fracture initiation. Moreover, the close agreement between the theoretically predicted values and the experimental data substantiates the validity and the potential use of the derived fracture criterion, i.e. Eq. 48. Designers may now use this criterion in order to predict failures in pressurized vessels by knowing only: the structural geometry, the crack length and the properties of the material.
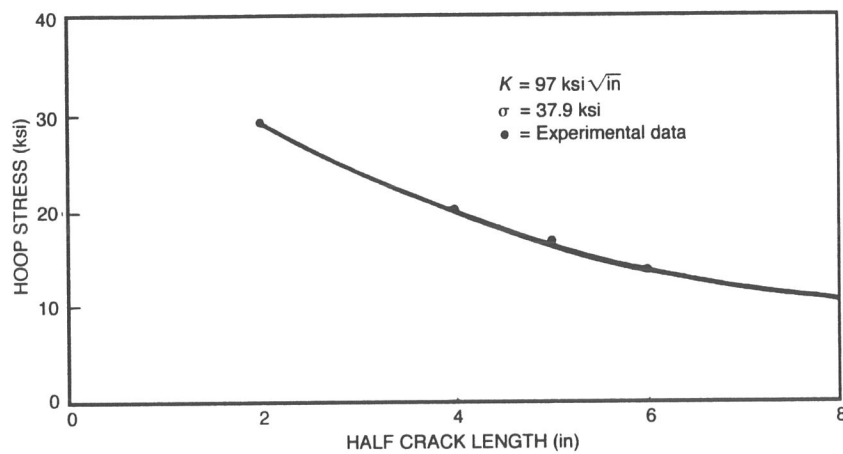

FIGURE 9. Comparison between theory and experiment for ABS-B steel spherical pressure vessels.

It may also be noted that the criterion may be used in two different ways. First, given a pressure vessel with certain geometrical parameters and a given internal pressure, one may deduce the critical crack length beyond which the vessel will fail catastrophically. For example, in the case of the Space Station, if a piece of debris impacted the manned module and penetrates it, then a hole with two adjacent wing cracks would be formed. This condition, most likely, will only cause leakage. However, if the formed cracks are sufficiently long so that the overall effective crack length is approximately equal to the critical crack length of the shell structure, then the module may unzip and thus fail catastrophically. Second, given a certain statistical flaw size, one may deduce the maximum safe internal pressure which can be sustained by the vessel. The latter, in particular, is useful in defining material specifications.

REFERENCES

1. Copley, L. G., Sanders, J. L., 1969. Longitudinal crack in a cylindrical shell under internal pressure, *Int. J. Fract.*, **5**, 117–131.
2. Do, S. H., and Folias, E. S., 1971. On the steady-state transverse vibrations of a cracked spherical shell, *Int. J. Fract.*, **7**, 23–27.
3. Dugdale, D. S., 1960. Yielding of steel sheets containing slits, *J. Mech. Phys. Solids*, **8**, 100–104.
4. Duncan, M. E., and Sanders, J. L., 1969. The effect of a circumferential stiffness on the stress in a pressurized cylindrical shell with a longitudinal crack, *Int. J. Fract.*, **5**, 133–155.
5. Erdogan, F., and Kibler, J., 1969. Cylindrical and spherical shells with cracks, *Int. J. Fract.*, **5**, 229–237.
6. Folias, E. S., 1964. The stresses in a spherical shell containing a crack. *ARL 64-23*. Aerospace Research Laboratories, U.S. Air Force, Dayton, Ohio.
7. Folias, E. S., 1965a. The stresses in a cracked spherical shell, *J. Math Phys.*, **5**, 327–346.
8. Folias, E. S., 1965b. A finite line crack in a pressurized spherical shell, *Int. J. Fract.*, **1**, 104–113.
9. Folias, E. S., 1967. A circumferential crack in a pressurized cylindrical shell, *Int. J. Fract.*, **3**, 1–11.
10. Griffith, A. A., 1924. The theory of rupture, *Proc. 1st Intern. Cong. on Appl. Mech.*, Delft, pp. 55–63.
11. Marguerre, K., 1938. Zur Theorie der gekrummten Platte grosser Formanderung, *Proc. 5th Intern. Congr. on Appl. Mech.*, pp. 93–101.
12. Sechler, E. E., and Williams, M. L., 1959. The critical crack length in pressurized monocoque cylinders. *Final Rept. GALCIT 96*, California Inst. of Tech. See also Williams, M. L., 1961, *Proc. Crack Propagation Symp.*, Cranfield, England, 1, pp. 130–165.
13. Kihara, H., Ikeda, K., and Iwanaga, H., 1966. Brittle fracture initiation of a line pipe. Document No. X-371-66, *Int. Inst. Welding*.
14. Anderson, R. B., and Sullivan, T. L., Fracture mechanics of through-cracked cylindrical pressure vessels, *NASA TN D-3252*.
15. Sopher, R. P., Lowe, A. L., Martin, D. C., and Tieppel, P. J., 1959. Evaluation of weld joint flaws as initiating points of brittle fracture, *Weld J. Res.*, **24**, 4415.

E. S. (TIM) FOLIAS

Tim Folias was born on 22 June 1936 in Thessaloniki, Greece. Upon the completion of his high school education, he came to the United States and attended the University of New Hampshire, where he received, in 1959, a B.S. degree in Electrical Engineering and, in 1960, a M.S. degree in Mathematics. He entered the graduate program at the Guggenheim Aeronautical Laboratory of the California Institute of Technology and completed his Ph.D. in Aeronautics (1963) with an emphasis in Solid Mechanics and Fracture.

Since 1966, Tim Folias has been a Professor at the University of Utah, with joint appointments in the Departments of Mechanical Engineering and Mathematics.

Professor Folias is known for his achievements in the theory of the structural integrity of pressurized vessels including the effect of double curvature, and 3D effects of shell thickness and composite structure.